On the Definition of a Risk Index based on Long-Term Metocean Data to Assist in the Design of Marine Renewable Energy Systems

Markel Penalba [1,3]*, Jose Ignacio Aizpurua[2,3], Ander Martinez-Perurena[1]

[1] *Fluid Mechanics Department, Mondragon University, Loramendi 4, 20500 Arrasate, Spain*

[2] *Signal Theory & Communications Department, Mondragon University, Loramendi 4, 20500 Arrasate, Spain*

[3] *Ikerbasque, Basque Foundation for Science, Euskadi Plaza 5, Bilbao, Spain*

Abstract

Marine Renewable Energy (MRE) systems are designed to maximise energy generation and ensure survivability. The traditional design process is based on pure environmental conditions, tends to be too conservative and limits the decision-making options. This paper presents a preliminary study on a novel risk-index combining the probabilistic occurrence matrix of sea-states with a consequence matrix. The stochastic direct sampling method is used for the quantification of occurrence matrices and consequences are estimated for fatigue effects and extreme loads. The paper shows a comparison of three design points (DPs) with increasing conservatism selected using metocean data for the period 1990-2000: high- and medium-risk DPs based on the novel risk index, and a low-risk DP obtained from a traditional PCA-based environmental contour. These DPs are compared to metocean data collected via *in-situ* measurements for the period 2000-2020, where the designed MRE system is supposed to operate. Results show that the low-risk DP overestimates the design H_s by 50%, while the high-risk DP underestimates it by 20%. The former would result in significant over-costs, while the later would very likely lead to catastrophic damages. The design H_s suggested by the medium-risk DP matches with the maximum H_s measured between 2000-2020, showing its suitability.

Keywords: **Marine Renewable Energy Design, Risk Index, Re-analysis metocean data, Environmental contours, Fatigue and Extreme loads.**

1. Introduction

Considering the ever-increasing worldwide energy demand and the undeniable environmental impact associated with the combustion of fossil fuels exposed in IPCC (2018), the

*Corresponding author

Email addresses: mpenalba@mondragon.edu (Markel Penalba [1,3]), jiaizpuruad@mondragon.edu (Jose Ignacio Aizpurua[2,3]), ander.martinezrd@alumni.mondragon.edu (Ander Martinez-Perurena[1])

energy transition towards a zero-emission energy system is one of the most crucial challenges of the mankind this century. In this transition, marine renewable energies can play a crucial role, *e.g.* IRENA (2019) estimates that installed offshore wind capacity is expected to multiply by 30, and this will require a massive change of scale for the sector in less than 30 years, at a speed unparalleled by the past development of other energy technologies. This rapid development of the sector leads to a proliferation of new opportunities and major challenges for the design of next generation cost-effective Marine Renewable Energy (MRE) systems.

Besides the economical perspective, the combination of a highly dynamic and harsh offshore environment (Adedipe et al. (2016)), ever-increasing rotor sizes and resulting loads (IRENA (2019)), and more powerful and frequent extreme events (Penalba et al. (2018)) makes the design of new solutions crucial for the MRE sector. In this sense, it is necessary to undertake the accurate characterisation of environmental conditions and evaluation of their impact on the different marine structures, which usually relies on pre-established design criteria included in various marine industry standards and guidelines, such as ISO (2015); DNV-GL (2017); NORSOK (2017) or IEC (2019).

These industry standards are generally based on joint metocean environment descriptions enabled by the availability of hindcast data. The metocean information of the last few decades is used to extract indicators for the determination of critical environmental loads, which enables the structure damage assessment during diverse conditions, from fatigue loads to extreme load rupture failures. However, the inference of these indicators is surrounded by different sources of uncertainty and this can result in overdesigned structures in order to avoid unexpected situations.

One of the most relevant and up-to-date industry standards in this specific case is IEC (2019), where design requirements for marine energy systems are detailed. The design process for MRE systems is defined as an iterative process where risk assessment plays an important role. The objective of the risk assessment is to provide further information about the previously mentioned uncertainties. In fact, the standard recommends defining consequences for different failures and combining them with the probability of the event or failure.

Hence, environmental conditions are divided into operational and extreme, defining a threshold wave height for each case. Once all relevant environmental conditions are determined, design load cases for each set of conditions are defined in order to evaluate the damage associated to each case: normal, extreme, abnormal, and transport and erection design categories, all purely based on environmental conditions. In addition, a set of limit states, *e.g.* ultimate limit state or fatigue limit state, are defined as limiting thresholds beyond which the MRE system fails to satisfy design requirements. In order to minimise the impact of the different sources of uncertainty, partial safety factors are suggested for each loading category, which intend to achieve a target safety level. However, these safety factors often add up to the already conservative techniques to estimate the extreme environmental conditions, resulting in significant over-engineering exercises.

If a MRE structures proofs to fulfil all the requirements, it is considered acceptable, leading to the beginning of the development stage.

1.1. Environmental contour modelling

One of the most popular approaches for the determination of extreme conditions oriented to the design of marine structures is the use of environmental contours. These contours define the boundary of sea-state conditions within a return period based on past metocean data. That way, the extreme structural loading and response analysis on the marine structure are limited to the sea-states lying on the contour, which significantly reduces the number of cases to be studied. In addition, this approach is particularly appealing due to its lack of dependency on any specific structure. Indeed, these environmental contours are included in most of the industry standards and guidelines ISO (2015); DNV-GL (2017); NORSOK (2017).

However, environmental contours provide just an approximation of the expected extreme events and, thus, should be used with care. Ross et al. (2020) review different techniques for the development of environmental contours, and suggest the potential applications of these contours and how to sensibly use them for each application.

In the environmental contour generation process, the first step is modelling the joint probability distribution of metocean variables that define the sea-state. The literature presents a number of different models which can be classified into two main groups: parametric and non-parametric models. For non-parametric models the kernel distribution is used, typically a multi-variate normal density function, where the maximum likelihood estimation method is used to fit the required kernel parameters. Although suitable for the description of the main body of a distribution, the description of distribution tails is highly sensitive to the kernel model parameters. Therefore, these parameters must be determined carefully. An example of this method is shown by Haselsteiner et al. (2017a) for the determination of extreme wind loads for an offshore wind turbine.

Similarly, parametric models can be used for the description of the contours. Copula models, considering that sea-states are defined as the combination of peak periods (T_p) and significant wave heights (H_s), allow for the definition of an inter-dependence between $\{T_p, H_s\}$ to describe the joint density distribution. The estimation of the copula model requires fitting the marginal distributions of T_p and H_s, and estimating the tail of these marginal distributions via extreme values models. Copulas have been widely used in the literature for diverse applications where different copula families have been suggested, *e.g.* Gaussian or 'max-stable', being the last model the most suited one for the description of the boundaries of metocean characteristics, as stated by Gudendorf and Segers (2010). More related to offshore engineering applications, Vanem (2016) demonstrates the need for asymmetric distributions in copula models, which are later used, for example, in Fazeres-Ferradosa et al. (2018) for the design of metocean data for offshore wind farms. An alternative to copula models are the hierarchical conditional models, where the dependence $\{T_p, H_s\}$ is represented as a product of densities. This partition allows for the use of simple distribution forms, such as the Weibull distribution presented in Bitner-Gregersen and Haver (1989). The combination of copulas and hierarchical representations is also suggested by Yu et al. (2014). Finally, conditional extreme models have also been suggested in the literature due to the need for determining boundaries of conditional distributions under different characteristics, as in Jonathan et al. (2010).

The different joint probability distributions of metocean variables are then used to estimate the environmental contours. These contours limit the extreme conditions that marine structures are likely to encounter within a pre-determined return period. The most significant method for the offshore engineering field is the inverse first-order reliability method (IFORM) that generates isodensity contours with a determined non-exceedance probability based on a hierarchical model, as suggested by Winterstein et al. (1993). Recently, this method has been generalised to include more appropriate elliptical contours by Lutes and Winterstein (2014) and extended from first- to second-order contours in Chai and Leira (2018).

Joint exceedance contours are also well-known approaches in ocean engineering, which represent a domain with an exceedance probability defined as a function of the return period by Gouldby et al. (2017). An issue of the IFORM method is that the probabilistic interpretation differs between the Gaussian and environmental spaces. In order to preserve the same statistical properties, a direct sampling (DS) method is suggested in Huseby et al. (2015), which has later been extended to 3-dimensional contours in Vanem (2017). Alternatively, Jonathan et al. (2014) proposes a method to generate joint exceedance contours where the pre-defined probability value is constant throughout the whole contour. One last approach that enables the definition of probabilistic contours via joint probability density functions is a method where isodensity contours are pre-defined. These isodensity contours can easily be associated to an exceedance probability, as demonstrated by Haselsteiner et al. (2017b).

All the statistical methods reviewed in this section provide a region where a MRE system where the system is likely to operate within a determined return period. However, each method can define a significantly different region, suggesting different H_s and T_p limits for the design of the MRE systems. The most suitable statistical method is demonstrated to vary with the geographical location of the area of study. Neary et al. (2020) study four different areas in the US, including data from 39 locations from all US coastal regions, and conclude that considering geographical variations in the wave resource is essential for an adequate selection of the contour method. As a basis for an objective and automated contour method selection, Neary et al. (2020) suggest that the most relevant geographical factor to be considered are the weather pattern (frequency and strength of seasonal storms) and local bathymetry (special interest is shown in shallow water areas). Hiles et al. (2019) also highlight the impact of geographical characteristics in the estimation of extreme events, where different statistically homogeneous regions were identified throughout the British Columbia, Washington and Oregon coasts. Authors also suggest the impact of the bathymetry on the development of extreme waves, with H_s limit varying from 17 m on highly exposed locations to 3.4 m at more sheltered locations. Overall, the authors conclude that different contours match well for $T_p < 20s$, while discrepancies arise for $T_p > 20s$. Similarly, the shape of the contour is shown to stretch upwards with higher mean H_s values.

1.2. Design criteria from contours

Regardless of the method used for its definition, environmental contours are modelled with the aim of estimating the extreme environmental loads that marine structures should be able to withstand within a pre-determined return period. In fact, the main motivation for the use of environmental contours in the design of marine structures is the determination of the most restrictive environmental conditions in a computationally efficient manner. That way, the response of the marine structure is estimated only for the extreme conditions determined by the contour, which significantly reduces the computational burden. The evaluation of the response has been carried out using diverse numerical and experimental approaches (see Coe et al. (2018)), which must be transformed into a domain of structural failure probability. The most basic approaches estimate the response of the structure as a function of the different environmental conditions via an accurately fitted statistical model, as in Gouldby et al. (2017). More complex procedures include reliability models that incorporate structural failure probability functions based on the exceedance of a given structural resistance.

The traditional process for marine structures is a *semi-automatised* process where the characteristics of the metocean conditions in a given location directly determine the design characteristics of the structure, as illustrated in Figure 1. First, data collected via *in-situ* measurements or hindcast climate models are used for the characterisation of metocean conditions, determining the operational $[X_{oper}(T_p, H_s)]$ and extreme environmental conditions $[X_{extr}(T_p, H_s)]$. Marine renewable energy systems are usually designed to produce under the operational mode and stop operating to reduce potential structural damages under survival mode, as illustrated in Figure 1. Thus, the response of the structure for operational $[R|X_{oper}(T_p, H_s)]$ and extreme conditions $[R|X_{extr}(T_p, H_s)]$ is evaluated, which are used to estimate the fatigue loads and extreme mechanical rupture loads, respectively. Finally, the design of the structure at different critical points is determined in order to withstand these loads. The extreme loads are the most critical events, which are typically based on environmental contours.

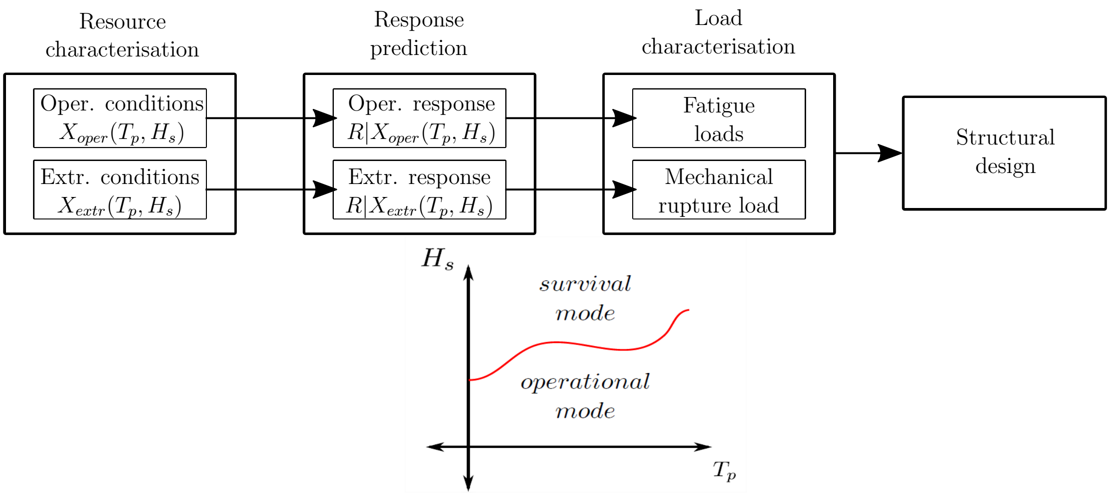

Figure 1: Traditional design workflow.

As a consequence, although post-processed via numerical response predictors, one can say that the decisions on the final design of marine structures are adopted solely based on pure metocean data from the contours. Furthermore, environmental contours include the boundary of the probabilistic analysis, but ignores the likelihood of these conditions and their consequences, hindering more advanced decision-making processes that may help preventing unintentional design conservatism.

In this context, the present paper presents a novel approach that combines the probability of extreme metocean conditions and the consequences on the structure to define a preliminary risk index to assist in the design of MRE systems.

The remainder of the paper is organized as follows. Section 2 presents the proposed risk index methodology, Section 3 defines the Case Study, Section 4 presents the results, Section 5 provides a discussion on the risk index and the main future lines to further develop this risk index, and Section 6 draws the main conclusions of the study.

2. Methodology

The proposed risk index ($\mathcal{R}$) is defined as the combination of the resource occurrence matrix ($\mathcal{X}$) and the consequence matrix ($\mathcal{C}$) which are defined independently and specifically for each location and MRE system, respectively. Figure 2 shows the proposed risk index approach.

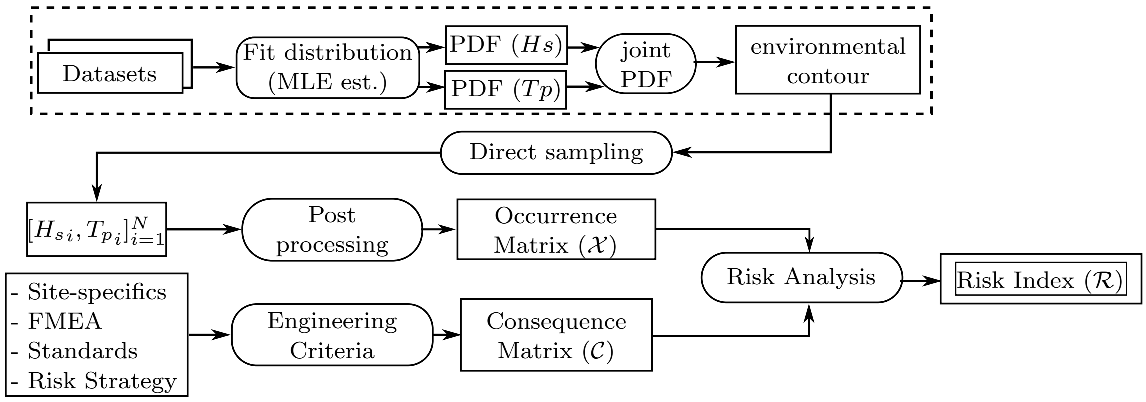

Figure 2: Risk Index definition flow chart.

The occurrence matrix defines the occurrence probability of a given sea-state within a given return period ($\mathcal{T}_r$). The consequence matrix quantifies the consequence criticality of the marine structure for each sea-state based on design criteria of industry standards and expert knowledge elicitation methods, such as failure modes and effects analysis (FMEA).

Both the inference of the occurrence matrix and the definition of the consequence matrix follow a systematic approach described in Section 2.1 and Section 2.2, respectively. Note that this paper presents a preliminary risk analysis framework that may be further complemented in future implementations. Refer to Section 5 for more insights on the potential improvements.

2.1. Future occurrence matrix determination

The occurrence matrix is inferred from the environmental contour, which defines the joint probability distribution of the pair $\{T_p, H_s\}$ conditioned on extreme events for a given return period. In turn, the environmental contour is defined using historical metocean data, which needs to be adequately organised as a joint $\{T_p, H_s\}$ probability density function (PDF).

2.1.1. Historical data

Historical metocean data for specific locations is usually provided by national or international oceanographic agencies, such as the NOAA (2021) *National Oceanic and Atmospheric Agency* in the Unites States or Puertos del Estado (2021) in Spain, which own sensing equipment in the areas of interest and *in-house* numerical models calibrated against these measurements. Hence, historical metocean data from different sources is typically employed, collected via either *in-situ* measurements as in Ruggiero et al. (2010), satellite altimeter measurements (see Young et al. (2011)), or atmospheric re-analyses of the *European Centre for Medium-Range Weather Forecasts* (ECMWF) as suggested by Bertin et al. (2013); Zheng et al. (2014); Reguero et al. (2015). In fact, the combination of measurements and re-analysis methods is also a typical procedure. For example, Ulazia et al. (2017); Penalba et al. (2018) use *in-situ* measurements, which serve as validation/calibration datasets for re-analysis datasets.

In the present paper, two different re-analysis datasets are used:

- *ERA5* is the latest global re-analysis of the ECMWF that covers the period from 1979 to the present (to be extended shortly) with a significant spatial and temporal resolution, 30 km and 1 hour, respectively. Stefanakos (2019) has recently proved that *ERA5* improves its previous versions developed by the ECMWF.

- *SIMAR* is an ensemble of modelling metocean data created upon a high-resolution numerical model by the Spanish Oceanographic Agency *Puertos del Estado*, which covers the coast along the Iberian Peninsula between 1958-2020 with a temporal resolution of 1 hour.

In addition, buoy-measurements provided by the Spanish Oceanographic Agency *Puertos del Estado* are used for the validation of the data from re-analyses. This validation is later shown in Section 3.1 using three statistical metrics (root mean square difference (RMSD), Pearson correlation coefficient and standard deviation) visualised through Taylor diagrams.

2.1.2. Environmental contours

The PDFs of a set of K data samples of wave height, $H = \{h_1, \ldots, h_K\}$, and wave period, $T = \{t_1, \ldots, t_K\}$, are fitted through the Maximum Likelihood Estimation (MLE) algorithm. The MLE estimates the best fitted parameters for the selected parametric distributions. In this case, the three-parameter Weibull PDF is used for the wave height, as suggested by Haselsteiner and Thoben (2020):

$$f_H(h) = (\frac{\beta}{\alpha})(\frac{h-\psi}{\alpha})^{\beta-1} exp(-((h-\psi)/\alpha)^{\beta}) \tag{1}$$

where ψ is the location parameter, α is the scale parameter and β is the shape parameter.

The PDF of the wave period is defined as a conditional distribution dependent on the PDF created for the wave height in (1). To this end, the log-normal distribution is fitted:

$$f_{T|H}(t|h) = \frac{1}{t\sigma\sqrt{2\pi}} exp(-\frac{(ln(t)-\mu)^2}{2\sigma^2}) \tag{2}$$

where μ is the expected value and σ is the standard deviation. The dependence between H and T is modelled by defining the expected value and the standard deviation in (2) as a function of H:

$$\mu(h) = E(ln(T)|H = h) \tag{3}$$

$$\sigma(h) = SD(ln(T)|H = h) \tag{4}$$

This dependency structure enables the integration of the both PDFs. The MLE algorithm estimates the optimal distribution parameters that minimize the error for the provided input data.

The joint PDF describes the joint probability of occurrence of wave height and period through the combination of (1) and (2):

$$f_{T,H}(t, h) = f_H(h) f_{T|H}(t|h) \tag{5}$$

By making use of environmental contour techniques it is possible to draw bounds on extreme events using various methods. This research focuses on the use of Monte Carlo methods to infer environmental contours through the DS approach presented in Bang Huseby et al. (2013) for the determination of the future occurrence matrix.

2.1.3. Direct sampling occurrence

The Monte Carlo sampling approach enables the probabilistic inference of N random variables of the pair $\{T_{p_i}, H_{s_i}\}_{i=1}^{N}$ from the parametric distributions learned from data for a given return period and conditioned on extreme events Bang Huseby et al. (2013). Every random variable pair $\{T_{p_i}, H_{s_i}\}$ is located in the 2-dimensional occurrence map and their occurrence counters are increased. This procedure is repeated for a high-number of trials (N=1e6 in this paper), and by the law of big numbers, the mean values of each of the points in the occurrence map indicate the probabilistic occurrence index for each pair of $\{H_{s_i}, T_{p_i}\}$. The occurrence matrix has been implemented using the `ViroCon` library in Python, as in Haselsteiner et al. (2019).

2.2. Consequence matrix determination

Environmental loads on marine structures can cause different damages ranging from minor fatigue degradation events to spontaneous and dramatic rupture of a component or part of the structure. These consequences are directly related to the environmental conditions and, thus, it should be possible to quantify the consequence for each sea-state based on the input load and the corresponding mechanical degradation effect. Ideally, this quantification should be supported by a FMEA that elicits expert knowledge to (i) identify failure cause-consequence relationships, (ii) develop experimental campaigns and (iii) implement numerical simulations.

If potential damages are divided into two main groups as in Coe et al. (2018), *i.e.* fatigue effects and extreme loads, consequences can also be quantified based on the criticality of these effects. For example, in the case of fatigue effects, loads are relatively low, but lead to structural damages due to cumulative effects. These cumulative effects are usually illustrated by means of stress-life (S-N) curves that depend on the load amplitude (see Figure 3 (a)), which is directly related to the wave height as in DNV-GL (2014). Therefore, it can be assumed that the impact of fatigue loads increases with wave height. However, this increase is not linear, meaning that the consequence criticality increases faster than the wave height (as an inverted S-N curve), as represented in Figure 3 (b).

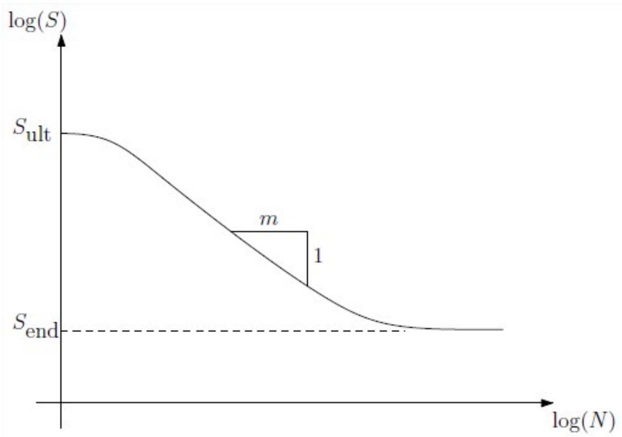

a) A typical S-N curve for cumulative fatigue effects Coe et al. (2018).

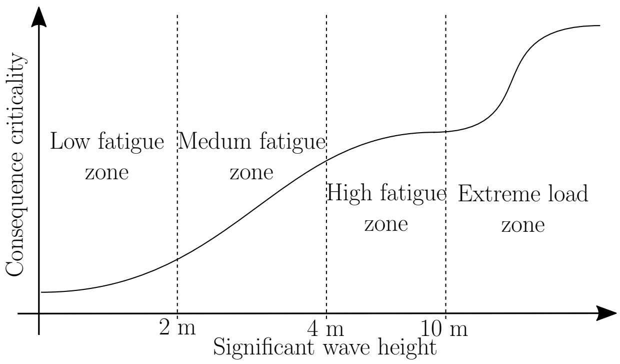

b) Consequences as a function of H_s.

Figure 3: Illustration of consequence variations.

Extreme loads may not be relevant for the analysis of the fatigue effects, but they are critical for the design of a marine structure. Therefore, the consequence criticality increases significantly in the *extreme load zone*, as illustrated in Figure 3 (b).

Hence, the preliminary consequence matrix defined in the present study (see Section 3.2) follows the trend outlined in Figure 3 (b) where only the impact of wave height is considered for the sake of simplicity. However, for a precise qualitative and quantitative analysis of the environmental consequences, relevant improvements should be incorporated into this preliminary consequence matrix. On the one hand, the impact of wave period must be included, since wave period is demonstrated to be a relevant parameter of environmental loading on marine structures. On the other hand, the consequence criticality should be defined upon an exhaustive reliability analysis, where a probabilistic analysis is considered for fatigue damage quantification, as by Horn and Leira (2019). Therefore, future developments of the risk index approach should include the effect of wave periods.

2.3. Risk index quantification

Once the occurrence and the consequence matrices are defined, the risk index can be calculated as follows,

$$\mathcal{R}(T_p, H_s) = X(T_p, H_s) \times \mathcal{C}(T_p, H_s), \tag{6}$$

where the dimensions of $\mathcal{R}$ are identical to X and $\mathcal{C}$, and indicates the risk of each pair of $\{T_{p_i}, H_{si}\}$ with respect to the structural integrity of the MRE system. High risk index values represent design requirements that should be considered, while low risk values represent requirements that could be neglected.

Hence, this risk index provides a deeper understanding of the design requirements by combining probabilistic environmental conditions of a given location within a selected return period with the potential consequences of each sea-state. Accordingly, the risk index will be able to:

i. warn the decision-makers of an area of low consequence criticality that, combined with high occurrence probability, should be considered on the design of the MRE system.

ii. dissuade the decision-makers from considering exaggerated design requirements that lead to excessively conservative design decisions.

3. Case study

For a preliminary analysis of the methodology presented in Section 2, a potential location for a MRE farm is considered in the Bay of Biscay. The necessary metocean data collected from *in-situ* measurements and atmospheric re-analyses are presented in Section 3.1, while a preliminary consequence matrix is created in Section 3.2.

3.1. Resource characterisation

The definition of the occurrence matrix requires a precise characterisation of the resource at the selected location, illustrated in Figure 4 (a). The three sets of metocean data described in Section 2.1.1 are compared in order to select the most appropriate one to build the occurrence matrix.

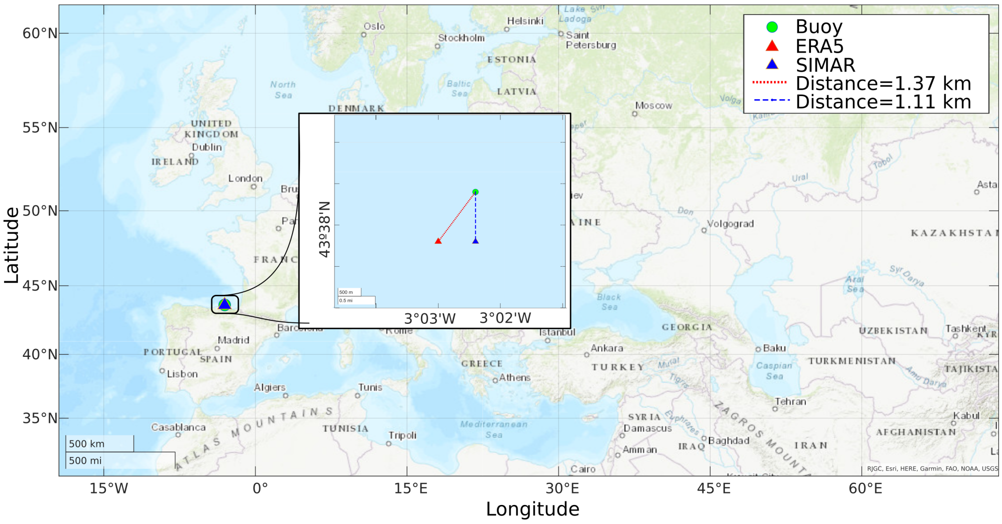

a) Geographical location of the different datasets.

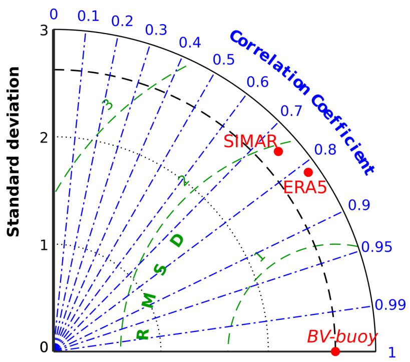

b) T_p Taylor diagram.

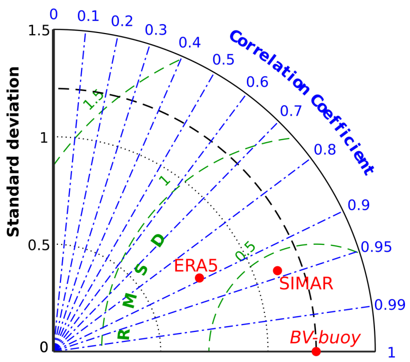

c) H_s Taylor diagram.

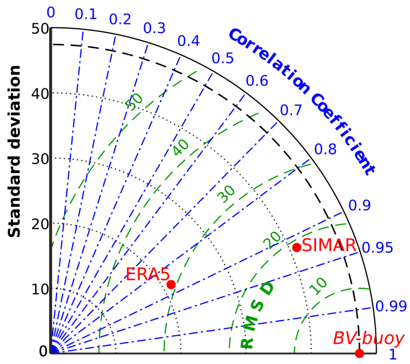

d) WEF Taylor diagram.

Figure 4: Metocean re-analysis data validation against the *BV-buoy*.

Table 1 presents the characteristics of each dataset, including the precise geographical location, period of time covered by the dataset, and mean T_p, H_s and wave energy flux (WEF), assuming that WEF is calculated combining H_s and energetic period (T_e) as follows,

$$WEF = 0.49\ H_s^2\ T_e, \tag{7}$$

where

$$T_e = \alpha\ T_p, \tag{8}$$

and $\alpha = 0.9$, as suggested in Tucker and Pitt (2001).

The data collected with the *in-situ* wave-measuring buoy *Bilbao-Vizcaya* that belongs to Puertos del Estado (*BV-buoy*) is considered as the ground-truth reference benchmark to compare and validate the other two datasets. To this end, the closest gridpoints of the *SIMAR* model (ID 3155039) and the *ERA5* reanalysis are studied, which are 1.11 km and 1.37 km away from the *BV-buoy*, respectively.

Table 1: Resource characteristics of the different datasets.

Dataset	Position (lon,lat)	Distance to buoy	Time Period	T_p (1990-2020)	H_s (1990-2020)	WEF (1990-2020)
BV-buoy	(-3.04°, 43.64°)	-	1990-2020	9.65	1.93	25.5
SIMAR (3155039)	(-3.04°, 43.63°)	1.11 km	1958-2020	10.23	1.73	25.3
ERA5	(-3.05°, 43.63°)	1.37 km	1979-2020	10.93	1.63	19.7

Although each datasets covers a different time period, the mean T_p, H_s and WEF values for each dataset presented in Table 1 correspond to the same time period (1990-2020), so that the results are comparable. Otherwise, the long-term variations of the wave conditions may bias the comparison.

In fact, Ulazia et al. (2017), Reguero et al. (2019) and Ulazia et al. (2020), among others, have demonstrated significant variations of the metocean conditions during the last decades, meaning that mean metocean parameters can significantly vary depending on the time interval considered in the analysis. In any case, the mean WEF lies between 18 and 25 kW/m for all the different datasets, which also matches with other values presented in the literature for the same area, such as Ulazia et al. (2017); Reguero et al. (2019); Ulazia et al. (2020).

Using the same time period for the three datasets, *i.e.* 1990-2020, results are comparable and conclusions on the suitability of each dataset can be drawn. On the one hand, *SIMAR* and *ERA5* datasets overestimate T_p and underestimate H_s and WEF. It should be noted that the underestimation of the H_s and WEF variables is a common issue for re-analysis datasets and wave models. Between the two datasets, the *ERA5* re-analysis shows a poorer performance, especially for the WEF variable, which is particularly poor at extreme events. In contrast, the *SIMAR* model shows relatively good agreement with *in-situ* measurements. In fact, the *SIMAR* model is specifically designed to accurately characterise the metocean conditions along the cost of the Iberian peninsula, while *ERA5* is a global model.

Figures 4 (b)-(d) illustrate the Taylor diagrams for T_p, H_s and WEF, respectively, where the coherency and correlation between the different datasets can be confirmed. As a consequence, the *SIMAR* and *ERA5* are considered to be validated against buoy measurements.

In the following, the *SIMAR* model is selected for the calculation of the occurrence matrix, because it covers the longest period of time and provides the best approximation to the buoy measurements.

3.2. A preliminary consequence matrix

In order to cover the main application sectors of the novel risk index presented in this paper, the consequence matrices for two reference MRE systems are suggested: The Corpower (2021) wave energy converter (WEC) and a generic floating offshore wind turbine (FOWT). In both cases, the consequence criticality curve illustrated in Figure 3 (b) underpins the consequence matrix, using the threshold between operational and survival modes illustrated in Figure 1 as a reference to define the limit between the fatigue zone and the extreme loading zone.

This threshold for the Corpower WEC is set to $H_s > 10$ m in De Andres et al. (2016), while $H_s > 4$ m is suggested for FOWTs in Moore et al. (2018). However, Collu and Borg (2016) states that the latter threshold is rather related to the maximum roll/pitch inclination angle of FOWTs, which prevents the system to operate correctly beyond 10° of inclination. Therefore, even if the power production is suspended when $H_s >4$ m, the extreme loading zone does not begin immediately after, resulting in a second zone of fatigue loads as a consequence of triggering the survival mode. In addition, the more aggressive operation of WECs caused by energy maximising control strategies (see Penalba and Ringwood (2019)) leads to higher fatigue loads on the structure and mooring lines due to slamming effects and higher motion amplitudes respectively. In turn, this situation results in a higher consequence criticality for the same H_s value. Therefore, the consequence criticality curves will diverge slightly for WECs and FOWTs. In any case, it should be noted that, ideally, a consequence matrix should be defined for each component, such as mooring lines, converter or platform structure, and power take-off elements and turbine blades.

The definition of the consequence criticality based on an inverted *S-N* curve, illustrated in Figure 3, is employed for the two MRE systems, as depicted in Figure 5 (a). Both the impact of fatigue effects (given as number of cycles before failure) and the consequence criticality are shown together in order to show their relationship. The initial number of cycles considered for WECs and FOWTs (5×10^6 and 6×10^6, respectively) are based on the standards defined in DNV-GL (2014), although this difference is indistinguishable in the consequence criticality due to the logarithmic scale. Therefore, a detail of the consequence criticality curves is shown for the region between 8-12s, where differences are most relevant.

Neglecting the impact of wave period on the criticality, the consequence matrices for WECs and FOWTs are shown in Figure 5 (b), where differences in lower H_s values are clearer, while the criticality is identical for higher H_s values. In order to obtain a risk index matrix in combination with the normalised occurrence matrix, the consequence criticality matrices are multiplied by the total number of sea-states (each sea-state being 1 hour long) considered along the standard MRE plant's lifetime of 20 years.

4. Results

After the definition of metocean data and the consequence matrix, the the different risk index matrices can be computed in order to determine the environmental characteristics to be employed in the design process. The analysis carried out in this section considers the decision-making instant in 2000 in order to design the MRE system to be deployed in the period between 2000-2020. This analysis permits defining training and testing datasets using different time intervals of historical metocean data between 1960-2000 provided by the *SIMAR* model, as well as the validation of design decisions for the period 2000-2020.

The historical time intervals are defined based on standards and recommendations of the different international organisations. The International Organization for Standardization (ISO) ISO (2015) suggests a historical record that covers the 25% of the return period of

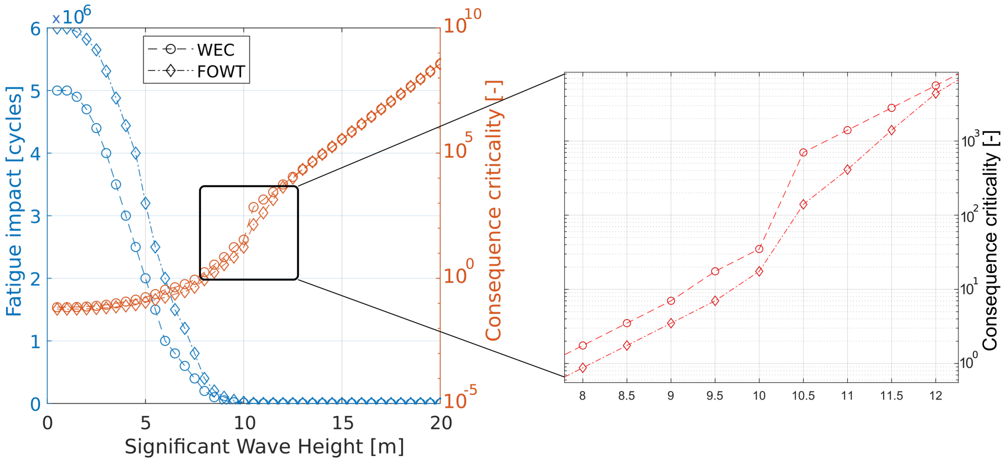

a)

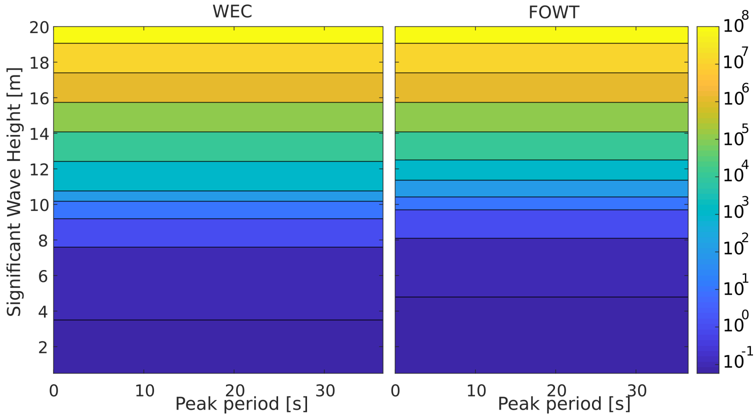

b)

Figure 5: Consequence vectors (a) and matrices (b) for WECs and FOWTs.

interest, which corresponds to 5, 12.5 and 25 years for return periods of 20, 50 and 100 years, respectively. In contrast, the Institute of Marine Engineering, Science & Technology (IMAREST) IMAREST (2018) recommends a longer period, preferably with over 30 years of metocean data, in order to accurately characterise extreme events. With respect to the return period recommended by these organisations, generally, IEC (2013) adheres to a 50-year return period for extreme design conditions, while API (1997) standards assume a 25-year, 50-year, or 100-year return periods for extreme events.

Hence, in order to cover the whole range of different recommendations and study the sensitivity of the risk index to both amount of historical input wave data and return period, three historical data intervals (10, 20 and 40 years going backwards from 2000) and three return periods (20-, 50- and 100-year) are studied, as schematically illustrated in Figure 6.

For the sake of simplicity, full results are only shown for the case where 10 years of historical metocean data is considered including the three return periods, synthesizing the sensitivity of the amount of input data later in this section.

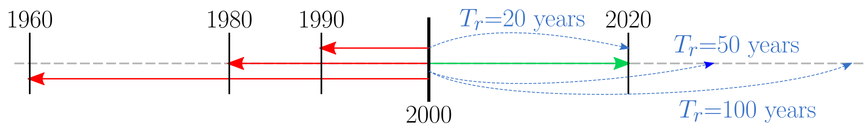

Figure 6: Analysed scenarios from the considered actual instant in year 2000.

As an illustrative example Figure 7 shows joint $\{T_p, H_s\}$ re-analysis data for the period 1990-2000, and the environmental contour and joint $\{T_p, H_s\}$ random variables estimated via DS for the period 2000-2020 with a return period of 50 years. Note that the re-analysis data points and DS-based random variables do not match because the DS contour is conditioned on a return period of 50 years, and DS-based random variables represent the whole range of values learned from the conditioned distribution. Due to the lack of physics-based modelling concepts, unlikely events may arise from the DS contour such as high-period estimations (above 30s), inferred from the low likelihood part of the learned probability distribution conditioned on a 50-year return period. This limitation may be addressed in future research through a fusion of physics-based and data-driven contour methods.

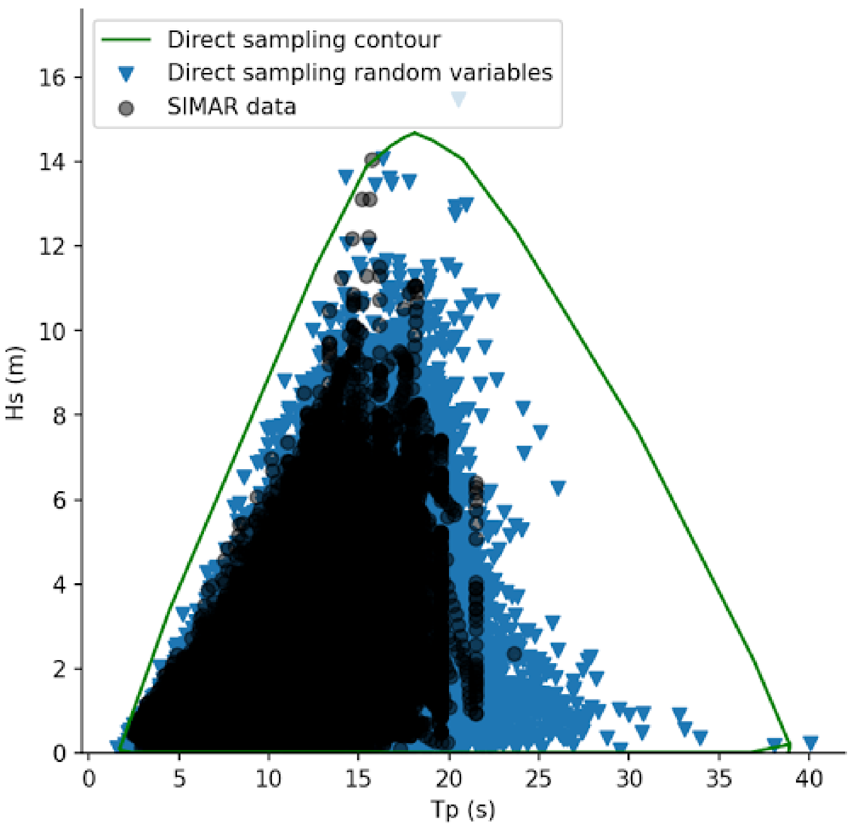

Figure 7: Environmental contour and estimated sea-states obtained via direct sampling for the period 2000-2020 for a return period of 50 years.

The novel methodology based on the risk index requires to compute the occurrence matrix for each return period, providing the information about extremes and the probability to encounter different sea-states. Figures 8 (a-c) show the DS-based future occurrence matrices given in percentage for the 20-, 50- and 100-years return periods, respectively. The most frequent sea-states are identical for the three cases, while the boundary of the occurrence area extends towards higher H_s and T_p values as return period increases, being the increase of the maximum H_s the most relevant for the design decision-making. Maximum H_s increases from 11.5 m for a return period of 20 years to 14 m with return periods of 50 and 100 years.

Figures 8 (d-f) and (g-i) illustrate the risk index matrices for FOWTs and WECs, respectively, which are generated following the method described in Section 2. In addition, similarly to the future occurrence matrices, the risk matrix is computed for the three return periods. These matrices are normalised with respect to the maximum risk value obtained in all the different simulations, so that a normalised risk index between 0 and 1 can be defined in order to easily identify the most critical areas for the design of MRE systems. The colour-code used in Figure 8 illustrates the highest risk in red, while the risk decreases as the colour turns blue.

All the risk index matrices illustrated in Figure 8 show very similar results with a repeated double peak pattern. The first peak is a smooth plateau-ish peak that appears in the high-occurrence area and corresponds to the most critical fatigue effects. In contrast, the second peak consists of a set of isolated peaks that correspond to unusual but devastating extreme events. That is exactly why, despite the very low occurrence of these extreme events, maximum risk index values ($\mathcal{R}_{MAX}$) appear in the area of the second set of peaks.

Differences between the type of MRE system are minor, but show a higher criticality of WECs due to their greater motion that results in more intense fatigue effects and extreme loads, as defined in Figure 5. These differences become more relevant when the return period varies, with $\mathcal{R}_{MAX}$ moving towards higher H_s, as expected. However, following the trend of the DS-based future occurrence matrices, variations of $\mathcal{R}_{MAX}$ between $\mathcal{T}_r = 50$ and $\mathcal{T}_r = 100$ appear to be significantly lower, although the area with a high risk is extended considerably from $\mathcal{T}_r = 50$ to $\mathcal{T}_r = 100$.

The same analysis is carried out for the three different time intervals of historical metocean data, using metocean data between 1980-2000 and 1960-2000 as inputs data for the computation of the risk index matrices. In parallel, environmental contours based on the principal components analysis (PCA) are also analysed. The PCA approach is selected because it is expected to provide more realistic representations of environmental contours under the extreme sea-state conditions, despite its higher sensitivity to the distribution fitting of the components, as stated in Eckert-Gallup et al. (2016); Wrang et al. (2021). However, future extensions of the proposed risk-index will also consider benchmarking the risk index against different environmental contour methods. Figure 9 illustrates the H_s corresponding to the $\mathcal{R}_{MAX}$ for all the cases analysed with the novel risk-index-based method.

Preliminary results show a low sensitivity of the risk-index-based method to the incorporation of different historical metocean data intervals. This lack of variation with respect to data intervals is particularly relevant for high return periods. However, inconsistent fluctuations of $\mathcal{R}_{MAX}$ at lower return periods indicate that the data processing methods may need to be revised, specially when handling very large datasets such as the metocean data

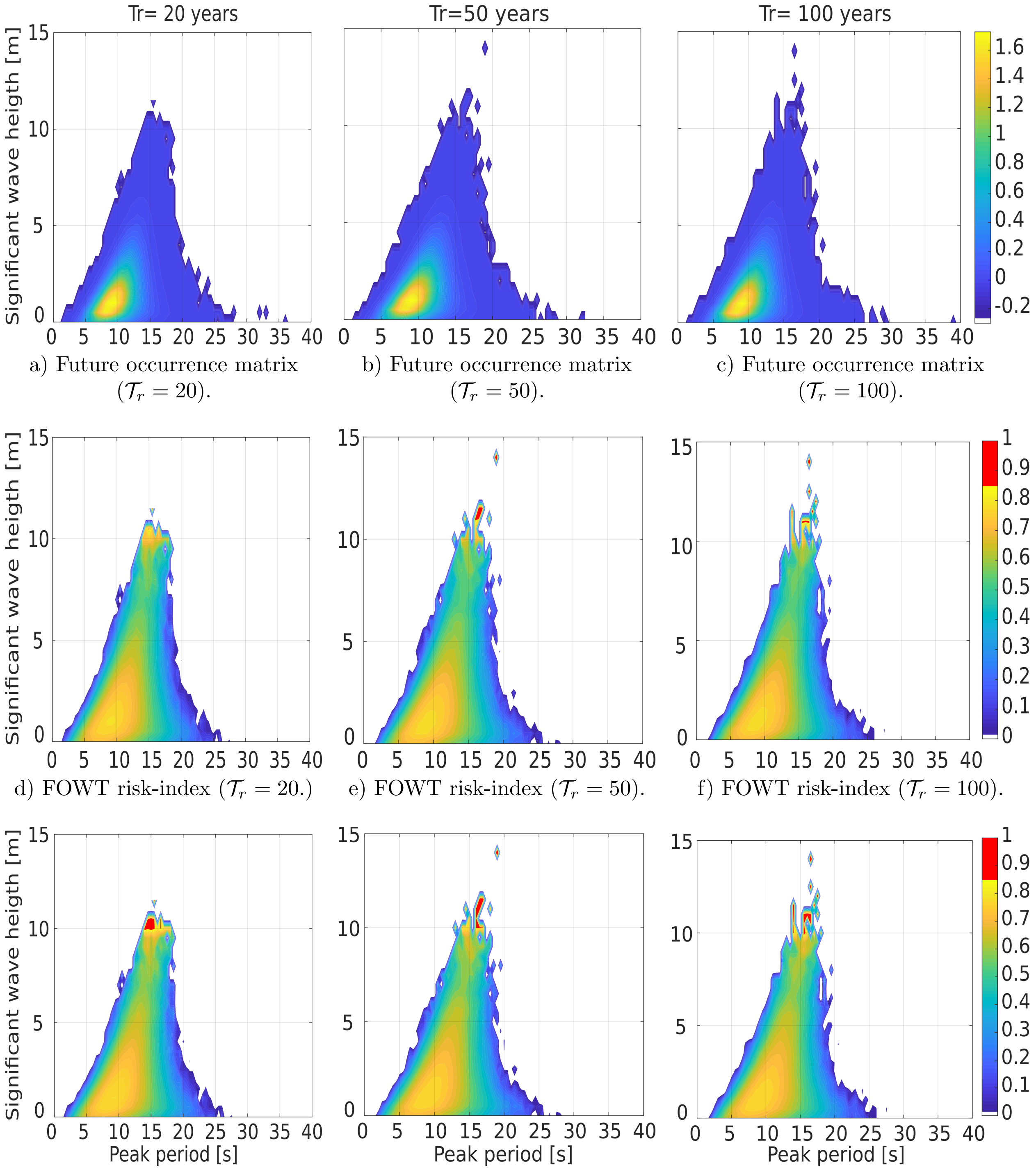

a) Future occurrence matrix ($\mathcal{T}_r = 20$).

b) Future occurrence matrix ($\mathcal{T}_r = 50$).

c) Future occurrence matrix ($\mathcal{T}_r = 100$).

d) FOWT risk-index ($\mathcal{T}_r = 20.$)

e) FOWT risk-index ($\mathcal{T}_r = 50$).

f) FOWT risk-index ($\mathcal{T}_r = 100$).

g) WEC risk-index ($\mathcal{T}_r = 20$).

h) WEC risk-index ($\mathcal{T}_r = 50$).

i) WEC risk-index ($\mathcal{T}_r = 100$).

Figure 8: Future occurrence matrix (a-c), and risk index matrices for FOWTs (d-f) and WECs (g-i).

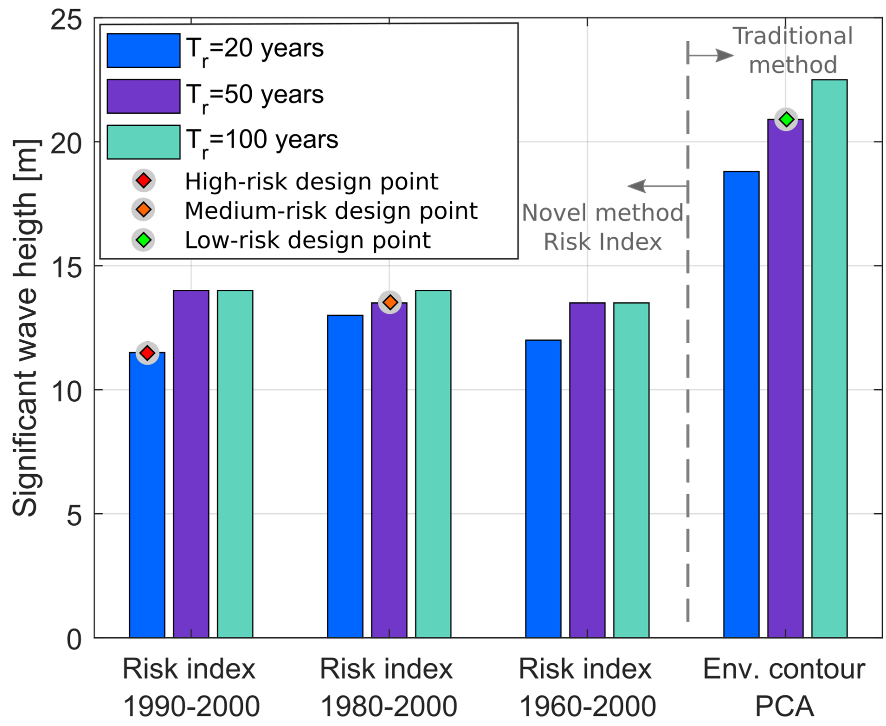

Figure 9: H_s for the $\mathcal{R}_{MAX}$ and maximum H_s for PCA-based environmental contours for the WEC case.

for the period 1960-2000.

The assumption of considering only metocean data for the period previous to 2000 allows for the assessment of the potential design points (DPs) by comparing them with the real resource characteristics measured during the virtual lifetime of the MRE system designed in 2000. Hence, this assessment is carried out for three potential DPs that consider different levels of conservativism for the design of a WEC, as highlighted in Figure 9: a high-risk DP based on the $\mathcal{R}_{MAX}$ computed using a decade of historical data between 1990-2000 and $\mathcal{T}_r = 20$ years, a medium-risk DP based on the $\mathcal{R}_{MAX}$ using two decades of historical data between 1980-2000 and $\mathcal{T}_r = 50$ years, and a highly conservative low-risk DP obtained from a pure PCA-based environmental contour using $\mathcal{T}_r = 50$ years. Table 2 describes the maximum H_s (H_s^{MAX}) considered in each case as the design reference to compute the maximum expected loads and define the structure that can survive these loads. Note that historical input data used for each DP is selected based on the recommendations by ISO (2015).

The metocean conditions for the period between 2000-2020, where the MRE plant deployed in 2000 would harvest energy, are provided by *in-situ* measurements of the *BV-buoy*. The boundary of these *in-situ* measurements is represented by green markers and a blue line, from where the maximum H_s value can be extracted ($H_s^{MAX^*} = 14.1m$). This $H_s^{MAX^*}$ is used as a reference value for the comparison of the different DPs. In addition, Figure 10 illustrates the joint $T_p - H_s$ data in red dots and the boundary corresponding to the period between 1990-2000, the environmental boundaries computed using this metocean data

Table 2: Design point characteristics.

DP	H_s^{MAX}	ΔH_s	Return period	Method
High-risk	11.5	-2.54 (-18.1%)	20-years	Risk-index
Medium-risk	13.8	0.16 (1.13%)	50-years	Risk-index
Low-risk	20.9	6.86 (48.9%)	50-years	PCA env. contour

with 20-, 50- and 100-years return periods, and the H_s limits of the three potential DPs. In principle, the three DPs described in Table 2 exceed significantly the maximum H_s of the period between 1990-2020, while the three environmental contours almost double that maximum value. However, models such as SIMAR and re-analysis data, in general, tend to underestimate extreme wave heights, as demonstrated by Campos et al. (2018), Rogowski et al. (2021) and de Alfonso et al. (2021), which studied, respectively, the South Atlantic Ocean, the North Atlantic Ocean and the Mediterranean coast. These underestimation needs to be carefully considered when computing either the risk index or environmental contour approaches to determine the design point for WECs and FOWTs.

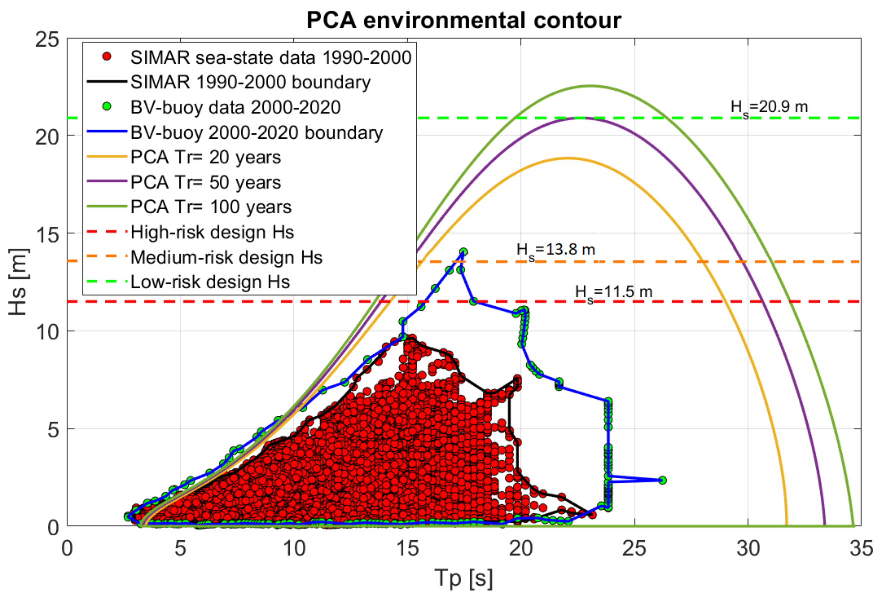

Figure 10: Historical joint $T_p - H_s$ data, PCA-based environmental contours with $\mathcal{T}_r = 20$, $\mathcal{T}_r = 50$ and $\mathcal{T}_r = 100$ for the period between1990-2000, the boundary of measured metocean data for the period 2000-2020, and the limiting H_s corresponding to the low-, medium- and high-risk DPs.

Figure 10 also shows the boundary of the measurements corresponding to the period 2000-2020 where the MRE plant designed following the different DPs is supposed to operate. This boundary extends well beyond the limits of the boundary corresponding to the period 1990-2000, meaning that the metocean conditions where the MRE plant operates are significantly harsher than the conditions used for the design. Therefore, it is shown that the high-risk DP underestimates the H_s design limit in about 2.5 m and 18%, resulting in an insufficient DP. The decision of taking that high risk would very likely result in catastrophic consequences for the MRE plant. In contrast, the low-risk DP would overestimate in 6.86 m and almost 50% the H_s design limit, resulting in an unnecessarily overdesigned marine structure leading to considerable over-costs. Finally, the medium-risk DP appears to provide the most appropriate H_s design limit that would result in an excellent compromise between ensuring survivability and reducing costs.

5. Discussion

Traditional MRE design methods solely based on environmental conditions may result in excessive conservatism due to the uncertainty of future metocean conditions, which are predicted via statistical and probabilistic methods. These methods, included in the most common industry standards, are based on the use of environmental contours that define the boundary of likely environmental conditions within a return period. The aim of this approach is the determination of the most extreme conditions that a marine structure should withstand within the lifespan of the device. Although different mathematical methods can be used for the determination of these contours, all are based upon pure metocean data, neglecting the likelihood of the most restrictive conditions and the consequences of these conditions. This may limit the decision-making process of design engineers by directly designing marine structures to survive to the most demanding metocean conditions identified in the environmental contours.

The novel risk-index-based method suggested in the present study aims to progress in two directions related to the design of MRE systems. On the one hand, the probabilistic estimation of the future metocean conditions. On the other hand, the determination of the structural consequences for each environmental condition, including fatigue effects and extreme mechanical rupture. That way, the risk index developed in this paper provides a more comprehensive information for the decision-making process, allowing engineers to take different levels of risk depending on the adopted strategy.

However, the proposed method may require further developments to be used in real design scenarios including the future resource characterisation and mechanical consequences. Similarly, an exhaustive analysis of the different sources of uncertainty may be important to improve the robustness of the method and adopt sensible decisions. Therefore, the results shown in the present paper should not be taken as final absolute results, but rather as figurative results that show the weak points of the traditional methods solely based on environmental conditions.

In this direction, these are some areas for potential improvement. On the one hand, improvements should arrive from a better characterisation of the future metocean conditions, including its non-stationarity. The more frequent and more powerful extreme events expected in the future could be incorporated, since any MRE system designed now will have to operate in and survive to future environmental conditions. To that end, first, the long-term wave trends observed in the literature and the impact of climate change should be identified appropriately, particularly on the enhancement of extreme events. Ensemble models that are able to assimilate long historical datasets and project assimilated historical trends into the future are highly valuable numerical tools. However, given the well-known inclination of wave models to underestimate extreme events, these models and re-analysis datasets should be carefully downscaled against *in-situ* measurements in order to minimise the uncertainty. Alternatively, long-term metocean data can be forecasted via Machine-Learning techniques once the most important characteristics of the historical dataset are carefully extracted, as suggested by A. Martinez-Perurena (2021).

On the other hand, an accurate determination of structural consequences must include all the most relevant effects that can damage marine structures. These effects include fatigue loads that should be accounted for via a stochastic analysis where the impact of wave period is crucial. Fatigue effects should be computed for the most frequent environmental conditions, combining the loads with the occurrence probability in order to compute their final impact. These effects can be computed with relatively simple numerical model, prioritising the computational burden over the simulation fidelity. In contrast, the impact of extreme events requires high-fidelity models, regardless of their computational requirements, where the highly-nonlinear breaking waves and green-water effects can be captured. Once the loads for the different effects are determined, the consequence of these loads must be quantified. To that end, a systematic procedure should be defined, defining the metric for the quantification, *e.g.* the inverse of the remaining cycles, and the mathematical framework to accumulate the impact of the different effects.

It should be noted that the presented risk index has been demonstrated here for offline MRE plant design decisions. However, it may be extended to an on-line risk monitor applied to other MRE-related applications such as maintenance operations.

6. Conclusions

The structural design of Marine Renewable Energy (MRE) systems must be optimised to maximise energy generation across a wide range of operational regions, ensure survivability under extreme events, and minimize costs. However, these requirements are often conflicting because surviving extreme events requires overdesigned structures that increase substantially their cost. In order to find a suitable compromise between survivability and cost, the precise characterisation of the metocean conditions and environmental loads is essential

However, the traditional design process solely based on environmental conditions tends to be too conservative and it lacks of flexibility for decision-making in the design process. Namely, extreme conditions are determined via probabilistic environmental contours for the determination of the most demanding loading conditions and accordingly, the MRE structure is designed. Due to the inherent conservatism of environmental contours, this design process results in excessively overdesigned and expensive structures.

In order to provide a deeper understanding of the design requirements, the present paper presents a preliminary study on a novel risk-index that combines a more appropriate probabilistic characterisation of the future metocean conditions and the consequences of the different metocean conditions on MRE structures. This way, the suggested risk index will provide the design engineers with comprehensive information about the design requirements by (i) warning them of an area of low-consequence criticality, but relatively high risk due to fatigue effects and (ii) dissuading design engineers from considering excessively conservative design.

The paper demonstrates the excessive conservatism of traditional design procedures via a comparative study of three design points (DPs) with increasing conservatism (high-risk DP based on the risk index, medium-risk DP based on the risk index, and low-risk DP based on a PCA-based environmental contour). The environmental-contour-based approach is demonstrated to overestimate the maximum H_s condition for the design by 50%, which would result in a significant over-costs of the MRE structure. In contrast, the flexibility provided by the novel risk-index approach enables design engineers to decide the level of risk they would like to take. The high-risk DP, for example, is shown to underestimate the design H_s, which would have been exceeded in real life in about 20%, very likely resulting in catastrophic damages on the structure. However, a more conservative decision, *i.e.* the medium-risk DP, would very precisely identify the maximum H_s value for the design, which would result in an excellent compromise between economical and technical aspects.

The marine resource is highly variable in multiple time-scales and it should be noted that different sources of uncertainties are present in the process. In fact, modelling and post-processing different sources of uncertainty may enhance the decision-making process and this is one of the areas for further development. In any case, although the risk-index approach suggested in this study still requires further development, the authors believe that it can assist in the decision-making process when designing MRE structures, avoiding excessive conservatism and achieving technically functional and economically attractive designs.

Acknowledgment

The authors gratefully acknowledge the Spanish agency Puertos del Estado for supplying metocean data from the SIMAR model and the Bilbao-Vizcaya measuring buoy. J. I. Aizpurua is funded by Juan de la Cierva Incorporacion Fellowship (Spanish State Research Agency - grant number IJC2019-039183-I).

References

M. Penalba J.I. Aizpurua A. Martinez-Perurena. Machine Learning based Long-Term Forecasting of Metocean Data for the Design of Marine Renewable Energy Systems. In *16th Conference on Sustainable Development of Energy, Water and Environment Systems (SDEWES), Dubrovnik, Croatia*, October 2021.

Oyewole Adedipe, Feargal Brennan, and Athanasios Kolios. Review of corrosion fatigue in offshore structures: Present status and challenges in the offshore wind sector. *Renewable and Sustainable Energy Reviews*, 61:141–154, 2016. ISSN 1364-0321. doi: https://doi.org/10.1016/j.rser.2016.02.017. URL https://www.sciencedirect.com/science/article/pii/S1364032116002252.

API. Supplement 1: Recommended Practice for Planning, Designing and Constructing Fixed Offshore Platforms: Load and Resistance Factor Design. Technical Report API RP 2A-LRFD-S1, America Petroleum Institute, Washington D.C., 1997.

Arne Bang Huseby, Erik Vanem, and Bent Natvig. A new approach to environmental contours for ocean engineering applications based on direct Monte Carlo simulations. *Ocean Engineering*, 60: 124–135, 2013. ISSN 0029-8018. doi: https://doi.org/10.1016/j.oceaneng.2012.12.034. URL https://www.sciencedirect.com/science/article/pii/S0029801812004532.

X. Bertin, E. Prouteau, and C. Letetrel. A significant increase in wave height in the North Atlantic Ocean over the 20th century. *Global and Planetary Change*, 106:77–83, 2013. doi: 10.1016/j.gloplacha.2013.03.009.

E. M. Bitner-Gregersen and S. Haver. Joint long term description of environmental parameters for structural response calculation. In *Proceedings of the 2nd International Workshop on Wave Hindcasting and Forecasting*, pages 25–28, 1989.

R. M. Campos, J. H.G.M. Alves, C. Guedes Soares, L. G. Guimaraes, and C. E. Parente. Extreme wind-wave modeling and analysis in the south Atlantic ocean. *Ocean Modelling*, 124(January):75–93, 2018. ISSN 14635003. doi: 10.1016/j.ocemod.2018.02.002. URL https://doi.org/10.1016/j.ocemod.2018.02.002.

Wei Chai and Bernt J. Leira. Environmental contours based on inverse SORM. *Marine Structures*, 60: 34–51, 2018.

Ryan G. Coe, Yi-Hsiang Yu, and Jennifer Van Rij. A Survey of WEC Reliability, Survival and Design Practices. *Energies*, 11(1), 2018. ISSN 1996-1073. doi: 10.3390/en11010004. URL https://www.mdpi.com/1996-1073/11/1/4.

M. Collu and M. Borg. 11 - Design of floating offshore wind turbines. In Chong Ng and Li Ran, editors, *Offshore Wind Farms*, pages 359–385. Woodhead Publishing, 2016. ISBN 978-0-08-100779-2. doi: https://doi.org/10.1016/B978-0-08-100779-2.00011-8. URL https://www.sciencedirect.com/science/article/pii/B9780081007792000118.

Corpower. Available in https://www.corpowerocean.com/, 2021.

Marta de Alfonso, Jue Lin-Ye, José M. García-Valdecasas, Susana Pérez-Rubio, M. Yolanda Luna, Daniel Santos-Muñoz, M. Isabel Ruiz, Begoña Pérez-Gómez, and Enrique Álvarez Fanjul. Storm gloria: Sea state evolution based on in situ measurements and modeled data and its impact on extreme values. *Frontiers in Marine Science*, 8:270, 2021. ISSN 2296-7745. doi: 10.3389/fmars.2021.646873. URL https://www.frontiersin.org/article/10.3389/fmars.2021.646873.

Adrian De Andres, Jéromine Maillet, Jørgen Hals Todalshaug, Patrik Möller, David Bould, and Henry Jeffrey. Techno-Economic Related Metrics for a Wave Energy Converters Feasibility Assessment. *Sustainability*, 8(11), 2016. ISSN 2071-1050. doi: 10.3390/su8111109. URL https://www.mdpi.com/2071-1050/8/11/1109.

DNV-GL. DNV-RP-C203: Fatigue design of offshore steel structures. Technical report, DET NORSKE VERITAS, 2014.

DNV-GL. DNV-RP-C205: ENVIRONMENTAL CONDITIONS AND ENVIRONMENTAL LOADS. Technical report, DET NORSKE VERITAS, 2017.

Aubrey C. Eckert-Gallup, Cédric J. Sallaberry, Ann R. Dallman, and Vincent S. Neary. Application of principal component analysis (PCA) and improved joint probability distributions to the inverse first-order reliability method (I-FORM) for predicting extreme sea states. *Ocean Engineering*, 112:307–319, 2016.

Tiago Fazeres-Ferradosa, Francisco Taveira-Pinto, Erik Vanem, Maria Teresa Reis, and Luciana das Neves. Asymmetric copula–based distribution models for met-ocean data in offshore wind engineering applications. *Wind Engineering*, 42(4):304–334, 2018. doi: 10.1177/0309524X18777323. URL https://doi.org/10.1177/0309524X18777323.

Ben Gouldby, David Wyncoll, Mike Panzeri, Mark Franklin, Tim Hunt, Dominic Hames, Nigel Tozer, Peter Hawkes, Uwe Dornbusch, and Tim Pullen. Multivariate extreme value modelling of sea conditions around the coast of England. *Proceedings of the Institution of Civil Engineers - Maritime Engineering*, 170(1): 3–20, 2017. doi: 10.1680/jmaen.2016.16. URL https://doi.org/10.1680/jmaen.2016.16.

G. Gudendorf and J. Segers. *Copula theory and its application (Ch. Extreme-value Copulas)*, volume 198, chapter Copula theory and its applications, pages 127–145. Springer, Berlin-Heidelberg, 2010.

Andreas F. Haselsteiner and Klaus-Dieter Thoben. Predicting wave heights for marine design by prioritizing extreme events in a global model. *Renewable Energy*, 156:1146–1157, 2020. ISSN 0960-1481. doi: https://doi.org/10.1016/j.renene.2020.04.112. URL https://www.sciencedirect.com/science/article/pii/S0960148120306443.

Andreas F. Haselsteiner, Jan-Hendrik Ohlendorf, Klaus-Dieter Thoben, and Klaus-Dieter Thoben. Environmental Contours Based on Kernel Density Estimation. In *13th German Wind Energy Conference (DEWEK), Bremen, Germany*, 2017a.

Andreas F. Haselsteiner, Jan-Hendrik Ohlendorf, Werner Wosniok, and Klaus-Dieter Thoben. Deriving environmental contours from highest density regions. *Coastal Engineering*, 123:42–51, 2017b. ISSN 0378-3839. doi: https://doi.org/10.1016/j.coastaleng.2017.03.002. URL https://www.sciencedirect.com/science/article/pii/S0378383916304446.

Andreas F. Haselsteiner, Jannik Lehmkuhl, Tobias Pape, Kai-Lukas Windmeier, and Klaus-Dieter Thoben. ViroCon: A software to compute multivariate extremes using the environmental contour method. *SoftwareX*, 9:95–101, 2019. ISSN 2352-7110. doi: https://doi.org/10.1016/j.softx.2019.01.003. URL https://www.sciencedirect.com/science/article/pii/S2352711018301420.

Clayton E. Hiles, Bryson Robertson, and Bradley J. Buckham. Extreme wave statistical methods and implications for coastal analyses. *Estuarine, Coastal and Shelf Science*, 223:50–60, 2019. ISSN 0272-7714. doi: https://doi.org/10.1016/j.ecss.2019.04.010. URL https://www.sciencedirect.com/science/article/pii/S0272771418301288.

Jan-Tore Horn and Bernt J. Leira. Fatigue reliability assessment of offshore wind turbines with stochastic availability. *Reliability Engineering & System Safety*, 191:106550, 2019. ISSN 0951-8320. doi: https://doi.org/10.1016/j.ress.2019.106550. URL https://www.sciencedirect.com/science/article/pii/S0951832018301492.

Arne Bang Huseby, Erik Vanem, and Bent Natvig. Alternative environmental contours for structural reliability analysis. *Structural Safety*, 54:32–45, 2015. ISSN 0167-4730. doi: https://doi.org/10.1016/j.strusafe.2014.12.003. URL https://www.sciencedirect.com/science/article/pii/S0167473014001143.

IEC. Design Requirements for Floating Offshore Wind Turbines. Technical report, International Electrotechnical Commission, Geneva, 2013. URL http://www.iec.ch/dyn/www/f?p=103:38:0::::FSP_ORG_ID,FSP_APEX_PAGE,FSP_LANG_ID,FSP_PROJECT:1282,23,25,IEC/TS%2061400-3-2%20Ed.%201.0.

IEC. IEC-TS-62600-2: Marine Energy - Wave, tidal and other water current converters. Part 2: Marine energy systems - Design Requirements. Technical report, International Electrotechnical Commission, Geneva, Switzerland, 2019.

IMAREST. Metocean Procedures Guide for Offshore Renewables. Technical Report 2, November, Institute of Marine Engineering, Science & Technology (OFFSHORE RENEWABLES SPECIAL INTEREST GROUP), 2018.

IPCC. Global Warming of 1.5$\circ$C. Technical Report ISBN 978-92-9169-151-7, Intergovernmental Panel on Climate Change (IPCC), 2018.

IRENA. Future of Wind: Deployment, investment, grid integration and socio-economic aspects (A Global Energy Transformation paper). Technical report, International Renewable Energy Agency, Abu Dhabi, 2019.

ISO. Petroleum and natural gas industries - Specific requirements for offshore structures - Part 1: Metocean design and operating considerations. Technical Report ISO 19901-1:2015, ISO, 2015.

P. Jonathan, K. Ewans, and J. Flynn. On the estimation of ocean engineering design contours. *Journal of Offshore Mechanics and Arctic Engineering*, 136(4), 2014. doi: 10.1115/1.4027645. URL https://www.scopus.com/inward/record.uri?eid=2-s2.0-84994372831&doi=10.1115%2f1.4027645&partnerID=40&md5=c6349e418229a2c507e63a6844faf0fa. cited By 18.

Philip Jonathan, Jan Flynn, and Kevin Ewans. Joint modelling of wave spectral parameters for extreme sea states. *Ocean Engineering*, 37(11):1070–1080, 2010. ISSN 0029-8018. doi: https://doi.org/10.1016/j.oceaneng.2010.04.004. URL https://www.sciencedirect.com/science/article/pii/S0029801810001022.

L Lutes and S Winterstein. Design contours for load combinations: Generalizing inverse form methods to dynamic problems. In *Proceedings of the 7th Computational Stochastic Mechanics Conference, Santorini, Greece*, pages 15–18, 2014.

Andy Moore, James Price, and Marianne Zeyringer. The role of floating offshore wind in a renewable focused electricity system for great britain in 2050. *Energy Strategy Reviews*, 22:270–278, 2018. ISSN

2211-467X. doi: https://doi.org/10.1016/j.esr.2018.10.002. URL https://www.sciencedirect.com/science/article/pii/S2211467X18300920.

Vincent S. Neary, Seongho Ahn, Bibiana E. Seng, Mohammad Nabi Allahdadi, Taiping Wang, Zhaoqing Yang, and Ruoying He. Characterization of extreme wave conditions for wave energy converter design and project risk assessment. *Journal of Marine Science and Engineering*, 8(4), 2020. ISSN 2077-1312. doi: 10.3390/jmse8040289. URL https://www.mdpi.com/2077-1312/8/4/289.

NOAA. National oceanographic and atmospheric agency. https://www.noaa.gov/, 2021.

NORSOK. NORSOK Standard N-003: Actions and Action Effects. Technical Report N-003, NORSOK, 2017.

M Penalba and J V Ringwood. Linearisation-based nonlinearity measures for wave-to-wire models in wave energy. *Ocean Engineering*, 171(November 2018):496–504, 2019. ISSN 00298018. doi: 10.1016/j.oceaneng.2018.11.033. URL https://doi.org/10.1016/j.oceaneng.2018.11.033.

Markel Penalba, Alain Ulazia, Gabriel Ibarra-Berastegui, John Ringwood, and Jon Sáenz. Wave energy resource variation off the west coast of Ireland and its impact on realistic wave energy converters' power absorption. *Applied Energy*, 224:205 – 219, 2018. ISSN 0306-2619. doi: https://doi.org/10.1016/j.apenergy.2018.04.121. URL https://www.sciencedirect.com/science/article/pii/S0306261918306895.

Puertos del Estado. Puertos del Estado. Available in http://www.puertos.es/es-es/oceanografia/Paginas/portus.aspx, 2021.

B. G. Reguero, I. J. Losada, and F. J. Méndez. A global wave power resource and its seasonal, interannual and long-term variability. *Applied Energy*, 148:366 – 380, 2015. ISSN 0306-2619. doi: http://dx.doi.org/10.1016/j.apenergy.2015.03.114.

B. G. Reguero, I. J. Losada, and F. J. Méndez. A recent increase in global wave power as a consequence of oceanic warming. *Nature Communications*, 10(205), January 2019. doi: https://doi.org/10.1038/s41467-018-08066-0.

Peter Rogowski, Sophia Merrifield, Clarence Collins, Tyler Hesser, Allison Ho, Randy Bucciarelli, James Behrens, and Eric Terrill. Performance assessments of hurricane wave hindcasts. *Journal of Marine Science and Engineering*, 9(7), 2021. ISSN 20771312. doi: 10.3390/jmse9070690.

Emma Ross, Ole Christian Astrup, Elzbieta Bitner-Gregersen, Nigel Bunn, Graham Feld, Ben Gouldby, Arne Huseby, Ye Liu, David Randell, Erik Vanem, and Philip Jonathan. On environmental contours for marine and coastal design. *Ocean Engineering*, 195:106194, 2020. ISSN 0029-8018. doi: https://doi.org/10.1016/j.oceaneng.2019.106194. URL https://www.sciencedirect.com/science/article/pii/S0029801819303798.

Peter Ruggiero, Paul D. Komar, and Jonathan C. Allan. Increasing wave heights and extreme value projections: The wave climate of the US Pacific Northwest. *Coastal Engineering*, 57(5):539–552, 2010.

Christos Stefanakos. Intercomparison of Wave Reanalysis based on ERA5 and WW3 Databases. In International Society of Offshore and Polar Engineers, editors, *Proceedings of the Twenty-ninth International Ocean and Polar Engineering (ISOPE) Conference, Honolulu, Hawaii, US*, June 2019.

M.J. Tucker and E.G. Pitt. *Waves in Ocean Engineering*. Elsevier Ocean Engineering Series. Elsevier Science, 2001. ISBN 9780080435664. URL https://books.google.es/books?id=0v5RAAAAMAAJ.

A. Ulazia, M. Penalba, G. Ibarra-Berastegui, J. Ringwood, and J. Saénz. Wave energy trends over the Bay of Biscay and the consequences for wave energy converters. *Energy*, 141, 2017. ISSN 03605442. doi: 10.1016/j.energy.2017.09.099.

Alain Ulazia, Ganix Esnaola, Paula Serras, and Markel Penalba. On the impact of long-term wave trends on the geometry optimisation of oscillating water column wave energy converters. *Energy*, 206:118146, 2020. ISSN 03605442. doi: 10.1016/j.energy.2020.118146. URL https://linkinghub.elsevier.com/retrieve/pii/S0360544220312536.

E. Vanem. 3-dimensional environmental contours based on a direct sampling method for structural reliability analysis of ships and offshore structures. In *Ships Offshore Struct*, 2017.

Erik Vanem. Joint statistical models for significant wave height and wave period in a changing climate. *Marine Structures*, 49:180–205, 2016. ISSN 0951-8339. doi: https://doi.org/10.1016/j.marstruc.2016.06.001. URL https://www.sciencedirect.com/science/article/pii/S095183391630106X.

Steven R. Winterstein, Todd C. Ude, C. Allin Cornell, Peter Bjerager, and Sverre Haver. Environmental parameters for extreme response: Inverse FORM with omission factors. In *Proc. 6th Int. Conf. on Structural Safety and Reliability, Innsbruck, Austria*, 1993.

Linus Wrang, Eirini Katsidoniotaki, Erik Nilsson, Anna Rutgersson, Jesper Rydén, and Malin Göteman. Comparative Analysis of Environmental Contour Approaches to Estimating Extreme Waves for Offshore Installations for the Baltic Sea and the North Sea. *Journal of Marine Science and Engineering*, 9(1), 2021. ISSN 2077-1312. doi: 10.3390/jmse9010096. URL https://www.mdpi.com/2077-1312/9/1/96.

I. R. Young, S. Zieger, and Alexander V. Babanin. Global trends in wind speed and wave height. *Science*, 332(6028):451–455, 2011.

H. Yu, J. Dauwels, and P. Jonathan. Extreme-Value Graphical Models With Multiple Covariates. *IEEE Transactions on Signal Processing*, 62(21):5734–5747, 2014. doi: 10.1109/TSP.2014.2358955.

Chongwei Zheng, Longtan Shao, Wenli Shi, Qin Su, Gang Lin, Xunqiang Li, and Xiaobin Chen. An assessment of global ocean wave energy resources over the last 45 a. *Acta Oceanologica Sinica*, 33(1): 92–101, 2014. ISSN 1869-1099. doi: 10.1007/s13131-014-0418-5.